Journal of Nuclear Materials 381 (2008) 297–301

Contents lists available at ScienceDirect

Journal of Nuclear Materials

journal homepage: www.elsevier.com/locate/jnucmat

In situ TEM study of cubic zirconia implanted with caesium ions

A. Gentils *, M.-O. Ruault, L. Thomé

CSNSM, CNRS-IN2P3-Université Paris-Sud, Bât. 104-108, 91405 Orsay, France

ARTICLE INFO

Article history:
Received 31 March 2008
Accepted 1 September 2008

PACS:
81.05.Je
68.37.Lp
61.72.Ff
61.80.Jh
61.72.Ww
82.80.Yc
61.85.+p

ABSTRACT

In situ transmission electron microscopy (TEM) observations were performed on yttria-stabilized zirconia during caesium (Cs) ion implantation at room temperature. Apparition of defect clusters is observed. The concentration of the latter increased with the Cs ion fluence. Until the higher fluence (2×10^{16} cm^{-2}), nothing else was observed except the overlapping of these defect clusters. At the higher fluence, Cs ion implanted thin sample was annealed between 600 and 1200 K. Only the recrystallization of cubic zirconia occurs during annealing; no other compounds were formed. The TEM results are compared to previous results obtained from Rutherford backscattering and channelling ion beam analysis techniques.

1. Introduction

Yttria-stabilized zirconia (YSZ) has potential uses as an inert matrix for plutonium utilisation and minor actinides disposition in nuclear reactors [1]. Indeed previous studies have shown that cubic YSZ is highly radiation resistant [2]. The most important radiotoxic elements resulting of the fission of actinides are ^{137}Cs and ^{90}Sr, which have half-lives up to 30 years. It has been shown that the damage produced by these fission products can be simulated experimentally by external ion irradiation [3].

One of the main questions concerns the nature of defects created in YSZ by low-energy ion irradiation. In the case of Xe ions, no amorphization have been observed in the YSZ matrix up to a level damage of 49 dpa, and a network of dislocations is present [4]. In the case of Sr, there was also no amorphization observed at a damage level of 200 dpa, but a layer of $SrZrO_3$ precipitates was found after the annealing of Sr ion implanted YSZ crystals [5,6]. In contrast, no precipitates were observed for Cs irradiation [6,8–11], in disagreement with thermodynamic modelling which predicts the formation of Cs_2ZrO_3 [7]. Only disordered areas and amorphization at high fluence have been found [8–10]; however, the amorphization level observed is not the same, it is higher from EPR experiments ($\geqslant 5 \times 10^{16}$ cm^{-2}) [10] and transmission electron microscopy (TEM) ($\geqslant 10^{17}$ cm^{-2}) [6,8] than from Rutherford backscattering and channelling (RBS/C) ones ($\geqslant 2 \times 10^{16}$ cm^{-2}) [9]. It has been also shown that Cs ion implantation in YSZ performed at 750 °C leads to the formation of dislocation loops [11], and that Cs is still present in the sample (the concentration of implanted Cs is below the solubility limit of 1.5 at.% of Cs in YSZ).

In the present work, we have studied the caesium behaviour in YSZ by *in situ* TEM to determine the microstructure after low-energy ion irradiation. Our study has been especially focused (i) on the evolution as a function of the fluence of the defects created by Cs ion implantation at room temperature and (ii) in a second part, post-annealing of the YSZ implanted at the highest Cs fluence studied was then performed, in order to study the ability of YSZ to confine radiotoxic elements such as Cs. The results are compared with those obtained previously by RBS/C techniques.

2. Experimental

Single crystals (⟨100⟩ orientation) of fully stabilized zirconia containing 9.5 mol% Y_2O_3 were used in the present study. Crystals were cut into plates to obtain TEM disc-specimen with a diameter of 3 mm and a thickness of 0.14 mm. Electron transparent specimens were prepared by dimpling and chemical thinning. Ion milling tests were done but a deformation of the thin sample was observed at low irradiation fluence, which worsens at higher fluence. These results convinced us to use chemical thinning, which has several advantages: (i) no potential artefacts due to defects induced by ion milling and (ii) a better resistance of the film to irradiation. A thin carbon layer (~0.7 nm) was deposited on the surface of the specimen to avoid charging effects during TEM experiments.

The Cs behaviour in YSZ was studied *in situ* with a Philips CM12 transmission electron microscope (120 kV) on-line with an

* Corresponding author. Tel.: +33 1 69 15 52 04; fax: +33 1 69 15 52 68.
E-mail address: Aurelie.Gentils@csnsm.in2p3.fr (A. Gentils).

0022-3115/$ - see front matter © 2008 Elsevier B.V. All rights reserved.
doi:10.1016/j.jnucmat.2008.09.002

ion-implanter [12]. This facility was available at CSNSM in Orsay, from 1980 to 2004. It is now updated through JANNuS (Joint Accelerators for Nanoscience, Nuclear and Simulation) facilities [13]. TEM samples were implanted at room temperature *in situ* in the microscope with increasing fluences of Cs^+ ions between 10^{14} and $10^{16}\,cm^{-2}$. The samples were tilted to about 7° with respect to the incident ion beam, in order to minimize ion channelling effects during the implantation. Low implantation currents, about $4 \times 10^{12}\,cm^{-2}\,s^{-1}$, were used in order to avoid any temperature rise of the sample during implantation. With an ion energy of 70 keV, the projected range is about ~20 nm below the free surface [14], which causes the defects associated with Cs to be formed mainly near the ion-entrance surface (sample thickness typically observed is ~60–80 nm), i.e., at the electron-exit free surface. We should also point out that the implantation and electron observations are not performed simultaneously but sequentially (see, e.g., [15]); the sample was alternately tilted to the ion beam for irradiation and to the electron beam for observation, as it is explained in details in [15]. Monte Carlo simulations with the SRIM code [14], assuming a threshold displacement energy of 40 eV for all elements, indicate that the number of dpa at the maximum of the defect distribution is about 10% higher for the same Cs fluence at 70 keV than at the energy used for RBS/C bulk samples (300 keV). In a second study, implanted YSZ TEM samples containing 5.8 at.% of Cs were annealed *in situ* in the microscope during 20 min at temperatures between 500 and 1100 K.

3. Results and discussion

3.1. Damage induced by Cs ion implantation

Until $2 \times 10^{14}\,cm^{-2}$, no extended defects (>1.5 nm) due to Cs ion irradiation is observed (Fig. 1(a)). Starting at a fluence of $3 \times 10^{14}\,cm^{-2}$ we note the apparition of small strained defect clusters ($\leqslant 5$ nm) (Fig. 1(b)). Until the final fluence of $10^{16}\,cm^{-2}$, the density of defect nano-clusters increases with an overlap of defect clusters above $10^{15}\,cm^{-2}$ (see Fig. 1(c)–(e)). Nano-clusters do not have characteristic contrasts of dislocations loops (black-white) situated near the free surface, but appear either full white, or full black, depending on their position on the same thickness fringes. This behaviour is typical of defect clusters, such as strained and very disordered areas, without preferred orientation. This observation is in agreement with the apparition of a weak diffuse ring on the diffraction pattern from a fluence of $3 \times 10^{14}\,cm^{-2}$ whose intensity increases with the fluence. Quantitative measurements of amorphization rate could have been performed with calibrated diffraction patterns of a same area and precise measurements of the greyscale obtained. This study could not be done due to the great difficulty to stay at the same place between each ion implantation steps during *in situ* experiments. It is important to note that relaxed amorphized zones could not really be observed by TEM imaging; indeed multiple amorphous states (relaxed and strained ones) have been previously observed in ion implanted Si and InP [12,16]. Strained amorphous zones appear such as high contrasted zones (white or black) due to the strain contrast, whereas a very weak contrast (grey zones) is observed for the relaxed amorphous zones. It has been also verified that no pronounced surface effects are observed between TEM experiments performed on ion implanted thick and thin samples. In both case the damage created by ion implantation is visible from the edge of the TEM foil over the depth. No denuded zone appear near the edge (i.e., in very thin parts, when the free surfaces are close), contrary to experiments in which the free surface plays a significant role (see, e.g., the defects induced in Si by self ion irradiation [17]). Since no surface effects exist in TEM thin foils, and since RBS/C experiments have shown no diffusion of the Cs in the sample [18], *in situ* TEM results can be compared to RBS/C results performed on bulk samples.

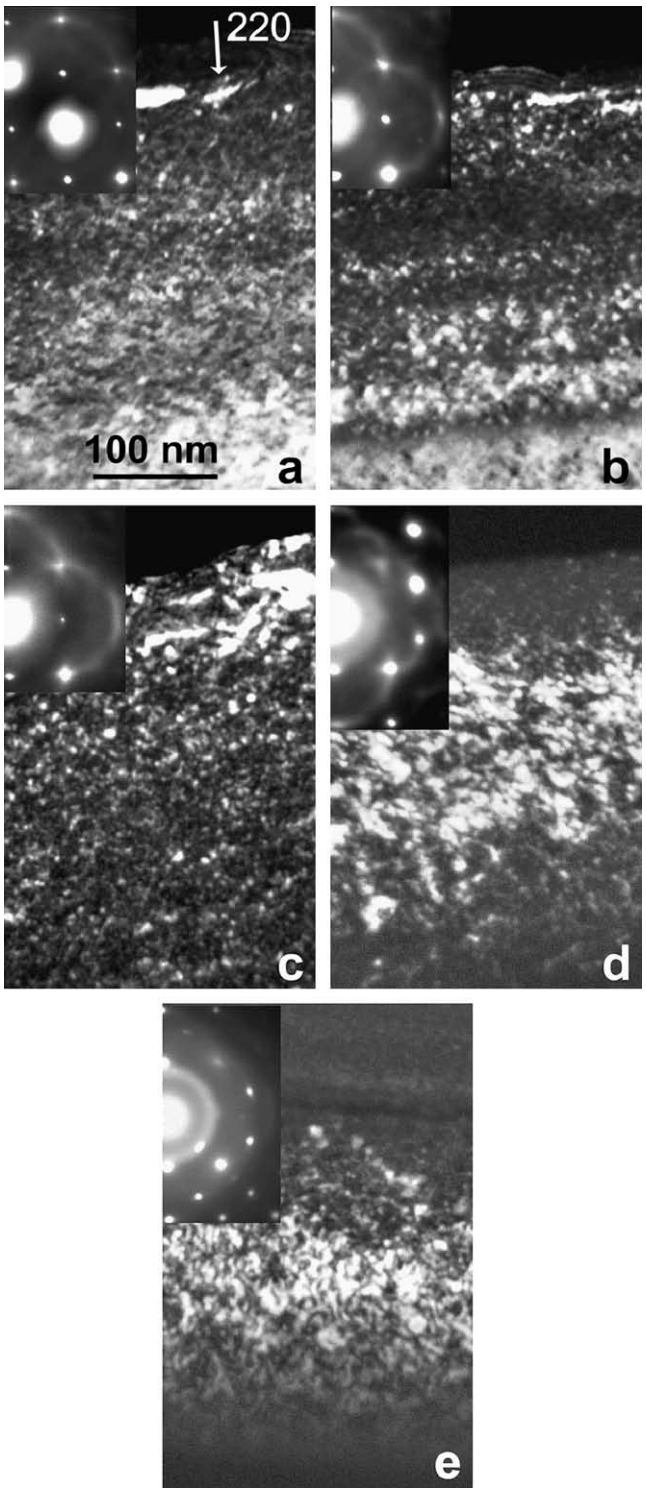

Fig. 1. Dark-field TEM micrographs showing the damage evolution of YSZ single crystals implanted at room temperature with 70 keV Cs ions at a fluence of (a) $2 \times 10^{14}\,cm^{-2}$ (0.6 dpa); (b) $3 \times 10^{14}\,cm^{-2}$ (0.9 dpa); (c) $10^{15}\,cm^{-2}$ (3.1 dpa); (d) $4 \times 10^{15}\,cm^{-2}$ (12.2 dpa) and (e) $10^{16}\,cm^{-2}$ (30.5 dpa). Diffraction patterns are shown in inset for each fluence. Since Cs ions were implanted from the direction opposite to that in which electrons were incident, the diffuse rings appear around diffracting spots in addition to the central spot.

In our previous RBS work [9,19] the amount of damage (f_D^{Zr}) created in the Zr sublattice of YSZ crystals by Cs irradiation was

measured as a function of the Cs fluence by *in situ* RBS/C experiments. A typical RBS/C spectrum registered in the ⟨100⟩-axial direction of a low-energy ion implanted single crystal displays a classical peak, called damage peak. This peak comprises two contributions: (i) the dechanneling fraction due to the distortion of atomic rows and planes induced by ion irradiation and (ii) the direct scattering contribution, whose distribution reflects the local concentration and the depth profile of Zr atoms displaced from their regular lattice positions by the bombarding Cs ions. The parameter f_D^{Zr}, also called damage level in the Zr sublattice, corresponds thus to the fraction of the Zr atoms displaced from their regular atomic positions. Fig. 2 shows the variation of the maximum of f_D^{Zr} (taken at the maximum of the damage peak) versus the number of displacement per atom of the target (dpa) induced by Cs ion irradiation. More information on how these results were obtained is given in Ref. [19]. This disordering kinetic exhibits three stages: (i) a first plateau characterized by a very low damage level at low dpa (i.e., low fluences); (ii) a sharp rise of f_D^{Zr} at 3 dpa and (iii) a slowly rising plateau above 4 dpa.

The first stage observed at low fluences in RBS/C experiments corresponds to the formation of isolated defect clusters seen by TEM, and the third stage observed at high fluences would correspond to the overlap of defect clusters. Stage 2, characteristic of the transition between these two stages, seems however to be too sharp to be explained only by the percolation of defect clusters. Thus the increase of the channelling yield occurring in stage 2 could be due to the combination of strains induced by the incorporation of Cs atoms in the crystalline structure and to the increase of the defect cluster density. The percolation of defect clusters would be enhanced by a collapse of the long-range order of the YSZ lattice. The structure of YSZ during stage 3 could be thus described by crystalline areas in a very disordered matrix.

At higher fluence (>10^{16} cm^{-2}, i.e., >30 dpa), the amount of damage created in the Zr sublattice measured by RBS/C is equal to one [20], meaning that the used YSZ single crystals are amorphized. This is in agreement with our results, and this amorphization at high fluence has been also observed by TEM in YSZ single crystals implanted with 10^{17} cm^{-2} Cs ions at room temperature [6,8].

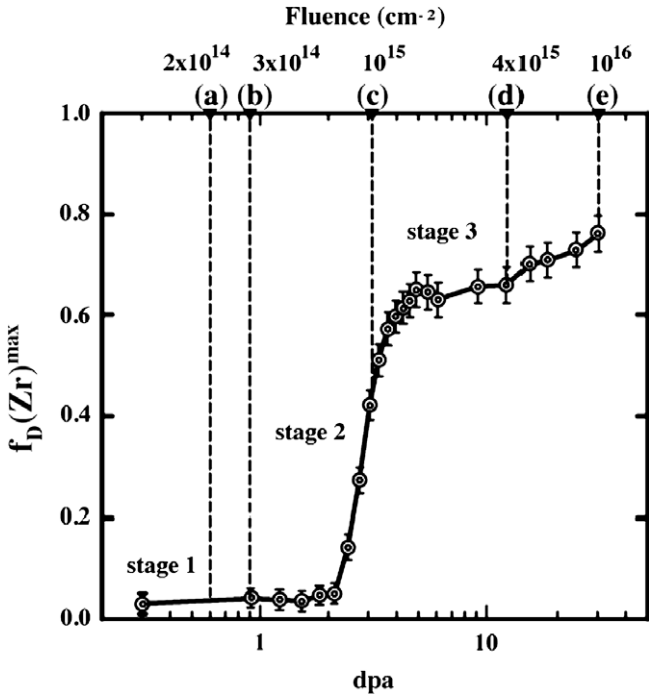

Fig. 2. Highest damage level in the Zr sublattice ($f_D(Zr)^{max}$) as a function of the number of dpa for YSZ single crystals implanted at room temperature with 300 keV Cs ions (obtained from RBS/C experiments) [19]. The letters correspond to the number of dpa for which the images of Fig. 1 have been taken.

Wang et al. [6,8] noted the presence of dislocation loops above a fluence of 2×10^{16} cm^{-2} for 70 keV Cs ions in thin cubic zirconia samples prepared by ion milling. This observation seems to be not coherent with an amorphization occurring at 10^{17} cm^{-2} observed by these authors [6,8] and confirmed recently by RBS measurements at 2×10^{16} cm^{-2} [20]. Note that dislocation loops were observed during implantation at high temperature (typically >700 K) [11].

The mechanism of amorphization of YSZ after Cs ion implantation is not completely clear. For a tentative explanation we should point out that:

(i) Cs precipitates are not formed, opposite to Sr ion implantation into YSZ [5,6]. In the latter, $SrZrO_3$ precipitates were observed after annealing without any amorphization. This result is attributed to the relatively small ionic size of Sr ions.

(ii) On the other hand, Cs is soluble in the YSZ matrix: up to 5.8 at.% has been measured in YSZ after a 10^{16} cm^{-2} Cs ion implantation at room temperature, significantly above the thermodynamic limit (1.5 at.% at 2000 K [7]). Since the radius of Cs atoms (in the Cs^+ oxidation state) is 1.65 Å, the substitution of a Zr atom by a Cs one creates a large stress in its vicinity. It has been shown that the stress relaxation may occur via the formation of a Cs-vacancy complex (i.e., Cs atom surrounded by oxygen vacancies) [21]. The fact that metastable system is created by ion implantation is well-known. It has been indeed previously shown that the impurity solubility is increased by using ion implantation to incorporate the impurity [22].

(iii) Moreover, due to the Cs ionic size, the presence of Cs in the matrix leads to a large strain in its vicinity [21], which could not lead alone to amorphization of YSZ. In fact, noble gas ion irradiation, such as Xe which has the same mass as Cs but which is electronically neutral (i.e., avoiding any chemical interaction with matrix atoms), leads to the creation of damage in the YSZ matrix, without any amorphization [4]. In case of Cs implantation, if we consider the electronic configuration of Cs ion, this situation will favor YSZ amorphization induced by Cs implantation. We can do a parallel with amorphization of Pd induced by semiconductor (e.g., Si) ion implantation [23].

It leads us thus to conclude that the electronic configuration of the Cs^+ ion plays an important role in the amorphization process of YSZ matrix.

3.2. Annealing

In order to identify if any phases were formed upon Cs migration, *in situ* TEM experiments were performed during thermal treatments on thin YSZ samples implanted at room temperature with 10^{16} cm^{-2} Cs ions, which provides a Cs concentration of 5.8 at.% at the peak maximum. The temperature was raised stepwise with 100 K intervals for half an hour from 500 to 1100 K. Up to 600 K we do not observe any noticeable change of the diffuse rings characteristic of the presence of very disordered areas (Fig. 3(a)–(c)). At 700 K the decrease of the amorphous ring intensity indicates a partial recrystallization which becomes significant above 800 K. At this temperature we observe the apparition of new spots randomly positioned on rings whose d_{hkl} correspond to ZrO_2 (Fig. 3(d)), in particular (111), (200), (220) and (311). Moreover EDX experiments show significant decrease in Cs concentration at 800 K. Thus recrystallization of ZrO_2 occurs during annealing, excluding any other phase precipitation. Polycrystallites where

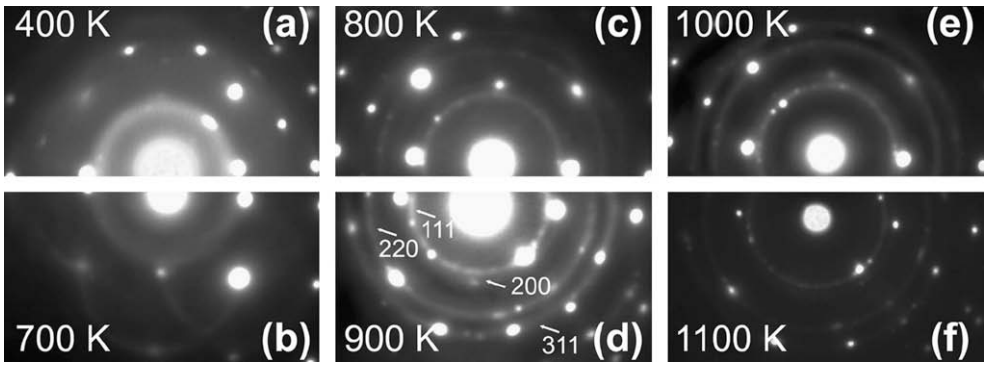

Fig. 3. Diffraction pattern of YSZ single crystals implanted with 5.8 at.% of Cs ions (10^{16} cm^{-2}, 70 keV) and annealed *in situ* in the microscope at the indicated temperatures. It is important to note that diffuse rings around secondary spots are due to the fact that the disordered zones are situated near the electron-exit surface.

imaged by means of dark fields taken on some dots taken on the (1 1 1) ZrO_2 dotted ring. Their average size is 6 nm. An increase of the number of recrystallized areas is observed (Fig. 4(a) and (b)) and corresponds to the apparition of additional spots, and the disappearance of diffuse rings.

A question arises from these results about the Cs presence in the matrix YSZ. In order to better understand the evolution of Cs atoms in that matrix and to monitor the Cs release, EDX experiments were performed with the same 100 K annealing intervals of half an hour from 500 to 1100 K on thin YSZ samples. EDX results, which provide a value of the Cs concentration in thin YSZ samples at each annealing step, are reported in Fig. 5. Measurements are averaged over the whole thickness of the foil (40–80 nm), so the total amount of Cs over the depth is measured. Release of Cs is observed at 800 K. At 1000 K the Cs concentration is stabilized around 2 at.%. For comparison, Fig. 5 also presents a summary of the results obtained by RBS on Cs-implanted YSZ bulk samples submitted to thermal treatments [9,18]. It shows the variation of the Cs concentration at the maximum of the distribution as a function of the annealing temperature for various implantation fluences. For crystals implanted at low atomic concentrations (below 1.5 at.%), no release of Cs atoms occurs up to the highest temperature investigated in this study. For crystals implanted at medium (~5 at.%) and high (~8 at.%) atomic concentrations, release of Cs atoms starts upon annealing at ~800 K. The result is a decrease in the Cs concentration down to a critical value of the order of 1.5 at.%. Furthermore, once the Cs concentration has dropped down to the critical concentration, the Cs depth profile remains almost unaffected up to the highest annealing temperature, revealing a high stability of YSZ implanted at low atomic Cs concentration. RBS experiments done in bulk samples show that release of Cs occurs at 800 K in YSZ, which is in good agreement with EDX results performed on thin samples. It shows again that there are no surface effects between thin and bulk samples. In conclusion, Cs is released from YSZ under annealing at 800 K and above, down to a critical value of ~1.5–2 at.%.

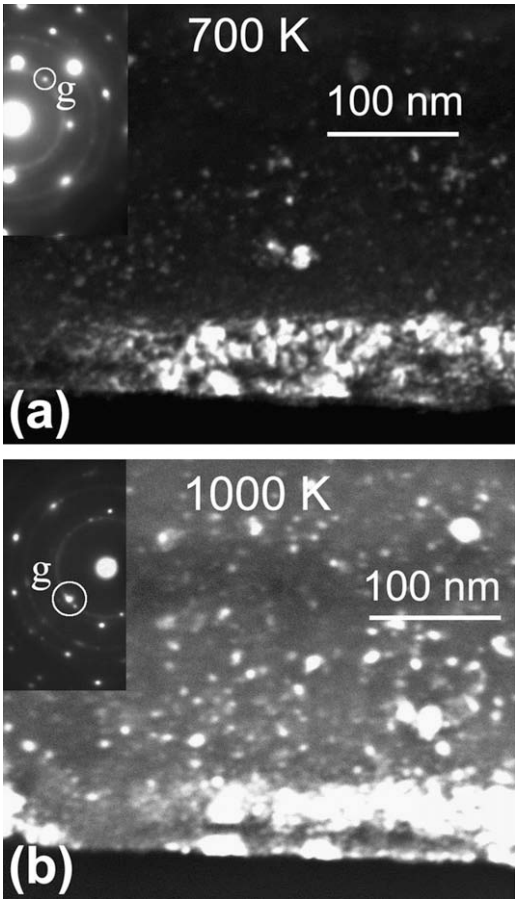

Fig. 4. Dark-field TEM micrographs and selected area diffraction patterns of YSZ sample implanted with 5.8 at.% Cs ions and annealed at (a) 700 and (b) 1000 K.

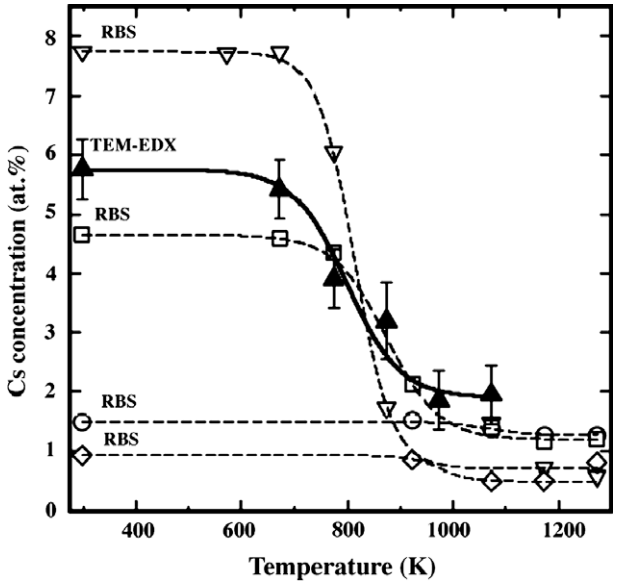

Fig. 5. Maximum Cs concentration vs. annealing temperatures for YSZ single crystals implanted with Cs ions at various fluences of 5×10^{15} cm^{-2} (diamonds), 10^{16} cm^{-2} (circles), 3×10^{16} cm^{-2} (squares) and 5×10^{16} cm^{-2} (inverted triangles). Open symbols: RBS results [18]; and filled triangles: TEM–EDX results.

In summary, diffraction patterns (Figs. 1 and 3) do not show the formation of a crystalline phase different from zirconia, neither after implantation, nor after thermal treatments until the final temperature studied. Indeed observed diffraction rings do not correspond to any Cs compound and are similar to those observed for the cubic structure of damaged zirconia. These results are not in agreement with thermodynamic calculations carried out by Pouchon et al. [7] on the Zr–Cs–O system, which suggest that the formation of ternary phases (such as Cs_2O–ZrO_2 and Cs_2ZrO_3) is possible between room temperature and 1170 K, with a solubility limit of 1.5 at.%. Nevertheless, if the size of Cs precipitates is very small (i.e., lower than 2 nm), they would not be observed in our experimental conditions.

In our case the solubility limit is increased, because Cs has been incorporated into the YSZ matrix by using ion implantation (see above). The Cs release is observed up to 900–1000 K along with a Cs limit concentration around 1.5–2 at.% after annealing at high temperature (cf. Fig. 5); it thus suggests that all the Cs is solid inside the matrix, and is released as a gas under annealing. Although it is not completely coherent with the Cs solubility limit obtained by thermodynamic calculations [7], we cannot exclude the possibility that a part of Cs forms small precipitates, invisible in our experimental conditions, and another part of gaseous Cs is released outside the matrix, as we have observed it. We should also point out that, during annealing, released Cs is gaseous, because a deposited layer of Cs has been indeed observed in the microscope excluding any more annealing experiment in the TEM up to 900–1000 K. In fact it was impossible to continue annealing experiment without adding Cs gas atoms in the vacuum of the microscope.

4. Conclusion

This study revealed the homogeneous apparition of defect clusters in YSZ during Cs ion implantation at room temperature. The number of strained and very disordered clusters (showing a high contrast) increases with the Cs ion fluence. Until the higher fluence studied, at room temperature, nothing else was observed except the overlapping of defect clusters. No precipitates were observed in any experimental conditions. The amorphization of YSZ is probably mainly induced by a 'chemical' effect due to the electronic configuration of Cs. During annealing only the recrystallization of cubic zirconia was seen; no other compounds were formed. In fact Cs solubility in YSZ was enhanced by ion implantation and gaseous Cs is released from the YSZ matrix during the thermal treatment. It is useful to note that RBS/C and TEM experiments are complementary, because RBS/C technique allows quantifying the disorder rate created by irradiation, whereas identification of defects was performed by *in situ* TEM.

Acknowledgements

We would like to acknowledge O. Kaitasov and S. Gautrot (CSNSM-Orsay) for technical assistance during *in situ* ion implantation. We are grateful to S. Collin (CSNSM-Orsay) and L. Mazerolles (CECM-Vitry) for discussions about the preparation of thin YSZ samples. This work is a part of the PhD Thesis of A.G. funded by Commissariat à l'Énergie Atomique (CEA) and Électricité de France (EDF). This work was partially supported by the GdR NOMADE.

References

[1] V.M. Oversby, C.C. McPheeters, C. Degueldre, J.M. Paratte, J. Nucl. Mater. 245 (1997) 17.
[2] C. Degueldre, J. Alloy Compd. 444&445 (2007) 36.
[3] F. Garrido, A. Gentils, L. Thomé, Surf. Coat. Technol. 196 (2005) 63.
[4] J. Cheng, F.B. Prinz, Nucl. Instrum. Meth. B 277 (2005) 577.
[5] S. Zhu, S.X. Wang, L.M. Wang, R.C. Ewing, X.T. Zu, Appl. Phys. Lett. 90 (2007) 171915.
[6] L.M. Wang, S.X. Wang, S. Zhu, R.C. Ewing, J. Nucl. Mater. 289 (2001) 122.
[7] M.A. Pouchon, M. Döbeli, C. Degueldre, M. Burghartz, J. Nucl. Mater. 274 (1999) 61.
[8] L.M. Wang, S.X. Wang, R.C. Ewing, Philos. Mag. Lett. 80 (2000) 341.
[9] A. Gentils, Effets d'irradiation et comportement des produits de fission dans la zircone et le spinelle, PhD Thesis, Université Paris-Sud, Orsay, France, 2003.
[10] X.T. Zu, S. Zhu, L.M. Wang, R.C. Ewing, J. Alloy Compd. 429 (2007) 25.
[11] L. Vincent, L. Thomé, F. Garrido, O. Kaitasov, Nucl. Instrum. Meth. B 257 (2007) 480.
[12] M.O. Ruault, J. Chaumont, H. Bernas, Nucl. Instrum. Meth. 209&210 (1983) 351.
[13] Y. Serruys, M.-O. Ruault, P. Trocellier, S. Henry, O. Ka, Ph. Trouslard, Nucl. Instrum. Meth. B 240 (2005) 124.
[14] J.P. Biersack, L.G. Haggmark, Nucl. Instrum. Meth. 174 (1980) 257.
[15] M.O. Ruault, F. Fortuna, H. Bernas, J. Chaumont, O. Ka, V.A. Borodin, J. Mater. Res. 20 (2005) 1758.
[16] H. Bernas, M.-O. Ruault, P. Zheng, Multiple amorphous states in ion implanted semiconductors (Si and InP), in: Coffa et al. (Eds.), Crucial Issues in Semiconductor Materials and Processing Technologies, Kluver Academic Publishers, Netherlands, 1992, p. 459.
[17] M.-O. Ruault, F. Fortuna, V.A. Borodin, M.G. Ganchenkova, M.A. Kirk, J. Appl. Phys. 104 (2008).
[18] A. Gentils, L. Thomé, J. Jagielski, F. Garrido, J. Nucl. Mater. 300 (2002) 266.
[19] L. Thomé, J. Fradin, J. Jagielski, A. Gentils, S.E. Enescu, F. Garrido, Eur. Phys. J. – Appl. Phys. 24 (2003) 37.
[20] L. Thomé, Private Communication CSNSM, Orsay, France, 2007.
[21] P. Villella, S.D. Conradson, F.J. Espinosa-Faller, S.R. Foltyn, K.E. Sickafus, J.A. Valdez, C.A. Degueldre, Phys. Rev. B 64 (2001) 104101.
[22] A. Traverse, M.-O. Ruault, L. Mendoza-Zelis, M. Schack, H. Bernas, J. Chaumont, L. Dumoulin, in: S.T. Picraux, W.J. Choyke (Eds.), Metastable Materials Formation by Ion Implantation, Materials Research Society, New York, 1982, p. 217.
[23] Lin Xi Wei, M.-O. Ruault, A. Traverse, H. Bernas, J. Less Common Met. 130 (1987) 133.